

# Onset Transition to Cold Nuclear Matter from Lattice QCD with Heavy Quarks to $\kappa^4$

---

**Jens Langelage\***

*Institute for Theoretical Physics, ETH Zürich, CH-8093 Zürich, Switzerland*

*E-mail: [ljens@phys.ethz.ch](mailto:ljens@phys.ethz.ch)*

**Mathias Neuman,† Owe Philipsen**

*Institut für Theoretische Physik, Goethe-Universität Frankfurt,*

*60438 Frankfurt am Main, Germany*

*E-mail: [neuman, philipsen@th.physik.uni-frankfurt.de](mailto:neuman, philipsen@th.physik.uni-frankfurt.de)*

We present results of our ongoing studies of an effective three-dimensional theory of thermal lattice QCD with heavy Wilson quarks. This is done by combined strong coupling and hopping parameter expansions. The full quark determinant of four dimensional lattice QCD is expanded in orders of the hopping parameter  $\kappa$ , the dimensional reduction is achieved by integrating over the spatial links. We present the calculation of the effective theory through order  $\kappa^n u^m$  with  $n + m = 4$ . This theory is then used to simulate heavy quarks near the cold and dense limit. For nonzero chemical potential the theory suffers from a sign problem, which is avoided by employing stochastic quantisation. Continuum extrapolated results for the onset of nuclear matter are shown and the region of convergence of the effective theory is discussed.

*31st International Symposium on Lattice Field Theory LATTICE 2013*

*July 29 - August 3, 2013*

*Mainz, Germany*

---

\*Speaker.

†Speaker

## 1. Introduction

Thermal lattice QCD suffers from a severe sign problem when chemical potential is nonvanishing. About a decade ago, several methods have been devised to circumvent this obstacle (see e.g. [1] and references therein), but these are only valid for  $\frac{\mu}{T} \lesssim 1$ . In order to go to higher chemical potentials, methods are required which at least potentially may solve this problem. Among these are Complex Langevin Dynamics (CLD) [2, 3], transformation of the degrees of freedom into so-called dual variables [4, 5] and the formulation of the theory on a Lefschetz thimble [6]. But even if these approaches finally succeed in solving the sign problem, it will remain very hard to study the region of cold and dense matter. This is because, in order to avoid the limiting artefact of saturation at finite lattice spacing, very fine lattices are required for high density, which implies in turn very large temporal lattice extents near  $T = 0$ . This motivates yet another approach, where we use strong coupling and hopping parameter expansions in order to simulate a 3d effective theory in a parameter regime where the sign problem is mild. See also [7, 8, 9, 10] for similar approaches, where staggered fermions are being used. There the strong coupling series is much harder to compute, but with the advantage that the chiral regime can be studied.

Here we show how to derive the 3-dimensional effective theory by integrating out the spatial degrees of freedom from the original  $(3 + 1)d$  theory. This procedure has the additional benefit that the effective action can be formulated in terms of complex numbers instead of group matrices. This allows us to simulate the effective theory quite fast and efficiently. Nevertheless, our approach also has some drawbacks, first and foremost that we do not know the effective action in the full parameter regime. Our strategy is to expand the effective action around the static strong coupling limit, i.e.  $\beta = \kappa = 0$ , in a combined strong coupling and hopping parameter expansion. In previous works [11, 12] this has been shown to work rather well and even allowing for continuum extrapolations in the heavy quark regime. Here, our approach is slightly adapted: In order to be able to describe physics near  $T = 0$  and large chemical potentials, we expand in  $\kappa$ , but keep in each order the complete dependence on chemical potential.

## 2. The effective action

We start on a  $(3 + 1)$ -dimensional lattice with Wilsons gauge and fermion actions, which after Grassmann integration may be written as

$$Z = \int [dU_\mu] \det[Q] \exp[S_g], \quad S_g = \frac{\beta}{2N_c} \sum_p [\text{Tr} U_p + \text{Tr} U_p^\dagger], \quad (2.1)$$

where we defined the quark hopping matrix as

$$Q_{\alpha\beta,xy}^{ab} = \delta^{ab} \delta_{\alpha\beta} \delta_{xy} - \kappa \sum_{\nu=0}^3 \left[ e^{a\mu\delta_{\nu 0}} (1 + \gamma_\nu)_{\alpha\beta} U_\nu^{ab}(x) \delta_{x,y-\hat{\nu}} + e^{-a\mu\delta_{\nu 0}} (1 - \gamma_\nu)_{\alpha\beta} U_{-\nu}^{ab}(x) \delta_{x,y+\hat{\nu}} \right].$$

Note that we consider only  $N_f = 1$  quark flavours in these first exploratory studies. The effective action is then defined by integrating out the spatial link variables

$$e^{S_{\text{eff}}} \equiv \int [dU_k] \det[Q] \exp[S_g]. \quad (2.2)$$

The crucial point of this approach is that the resulting effective theory does not depend on the single temporal link variables, but only on their product along a temporal axis, i.e. the Polyakov loops

$$L_i \equiv \text{Tr} W_i \equiv \prod_{\tau=1}^{N_\tau} U_0(\vec{x}_i; \tau) . \quad (2.3)$$

Our goal is now to expand eq. (2.2) in a combined strong coupling and hopping parameter expansion. This introduces an infinite tower of effective interaction terms, which will be ordered according to their leading powers in  $\beta, \kappa$ . We will also make sure that we have the complete dependence on chemical potential in each order of the hopping parameter expansion, starting with the zeroth order, which is simply pure gauge theory.

## 2.1 Pure gauge theory

In case of pure gauge theory it is advantageous to perform a character expansion

$$\exp \left[ \frac{\beta}{2N_c} (\text{Tr} U + \text{Tr} U^\dagger) \right] = c_0(\beta) \left[ 1 + \sum_{r \neq 0} d_r a_r(\beta) \chi_r(U) \right] , \quad (2.4)$$

where the factor  $c_0(\beta)$  can be neglected as it is independent of gauge links and cancels in expectation values. In earlier publications [11, 13, 14], we have shown how to compute the effective gauge theory up to rather high orders in the fundamental character expansion coefficient  $u(\beta) \equiv a_f(\beta)$ . In leading order we have a chain of  $N_\tau$  fundamental plaquettes winding around the temporal direction and closing via periodic boundary conditions. It reads

$$e^{S_{\text{eff}}^{(1)}} = \lambda(u, N_\tau) \sum_{\langle ij \rangle} (L_i L_j^* + L_i^* L_j) , \quad \lambda(u, N_\tau) = u^{N_\tau} [1 + \dots] , \quad (2.5)$$

where higher order corrections of  $\lambda(u, N_\tau)$  as well as a discussion of higher order interaction terms can be found in [13]. In the leading order expression of eq. (2.5) we already see that  $\lambda(u, N_\tau)$  is suppressed for large  $N_\tau$ , since  $u < 1$ , see also [11] for a further discussion of this aspect.

## 2.2 Static quark determinant

Let us now expand the quark determinant in a hopping expansion. In order to keep the complete dependence on chemical potential, we split the quark matrix according to

$$Q = 1 - T - S = 1 - T^+ - T^- - S^+ - S^- , \quad (2.6)$$

in positive and negative temporal and spatial parts. The static determinant is then given by neglecting the spatial parts. We define and compute the static determinant to be

$$\begin{aligned} \det[Q_{\text{stat}}] &= \det[1 - T] = \det[1 - T^+ - T^-] \\ &= \det \left[ 1 - \kappa e^{a\mu} (1 + \gamma_0) U_0 \delta_{x,y-\hat{0}} - \kappa e^{-a\mu} (1 - \gamma_0) U_0^\dagger \delta_{x,y+\hat{0}} \right] \end{aligned} \quad (2.7)$$

with propagation in the temporal direction only. Performing the space and spin determinant we get

$$\det[Q_{\text{stat}}] = \prod_{\vec{x}} \det \left[ 1 + (2\kappa e^{a\mu})^{N_\tau} W_{\vec{x}} \right]^2 \det \left[ 1 + (2\kappa e^{-a\mu})^{N_\tau} W_{\vec{x}}^\dagger \right]^2 . \quad (2.8)$$

A well-known relation valid for  $SU(3)$  then allows us to reformulate this in terms of traced Polyakov loops

$$\det[Q_{\text{stat}}] = \prod_{\vec{x}} \left[ 1 + cL_{\vec{x}} + c^2 L_{\vec{x}}^\dagger + c^3 \right]^2 \left[ 1 + \bar{c}L_{\vec{x}}^\dagger + \bar{c}^2 L_{\vec{x}} + \bar{c}^3 \right]^2, \quad (2.9)$$

with  $c = c(\mu) = (2\kappa e^{a\mu})^{N_\tau} = \bar{c}(-\mu)$  in the strong coupling limit.

### 2.3 Kinetic quark determinant

In order to compute a systematic hopping expansion, we define the kinetic quark determinant as follows

$$\begin{aligned} \det[Q] &\equiv \det[Q_{\text{stat}}][Q_{\text{kin}}], \\ \det[Q_{\text{kin}}] &= [1 - (1 - T)^{-1}(S^+ + S^-)] \equiv \det[1 - P - M] = \exp[\text{Tr} \ln(1 - P - M)], \end{aligned} \quad (2.10)$$

which we then split into parts describing quarks moving in positive and negative spatial directions,  $P = \sum_k P_k$  and  $M = \sum_k M_k$ . The reason for this is that the trace occurring in eq. (2.10) is also a trace in coordinate space. This means that only closed loops contribute and hence we need the same number of  $P$ s and  $M$ s in the expansion of the logarithm. Through  $\mathcal{O}(\kappa^4)$  we have

$$\begin{aligned} \det[Q_{\text{kin}}] &= \exp \left[ -\text{Tr} PM - \text{Tr} PPMM - \frac{1}{2} \text{Tr} PMPM \right] [1 + \mathcal{O}(\kappa^6)] \\ &= \left[ 1 - \text{Tr} PM - \text{Tr} PPMM - \frac{1}{2} \text{Tr} PMPM + \frac{1}{2} (\text{Tr} PM)^2 \right] [1 + \mathcal{O}(\kappa^6)]. \end{aligned} \quad (2.11)$$

The next step is now to consider the different directions in  $P$  and  $M$  and to neglect the vanishing contributions, i.e. those which have e.g. a  $P_k$  but no  $M_k$

$$\sum_{kl} \text{Tr} P_k M_l = \sum_k \text{Tr} P_k M_k, \quad (2.12)$$

$$\sum_{klmn} \text{Tr} P_k P_l M_m M_n = \sum_k \text{Tr} P_k P_k M_k M_k + \sum_{k \neq l} \text{Tr} P_k P_l M_k M_l + \sum_{k \neq l} \text{Tr} P_k P_l M_l M_k, \quad (2.13)$$

$$\frac{1}{2} \sum_{klmn} \text{Tr} P_k M_l P_m M_n = \frac{1}{2} \sum_k \text{Tr} P_k M_k P_k M_k + \frac{1}{2} \sum_{k \neq l} \text{Tr} P_k M_k P_l M_l + \frac{1}{2} \sum_{k \neq l} \text{Tr} P_k M_l P_l M_k, \quad (2.14)$$

$$\frac{1}{2} \sum_{klmn} \text{Tr} P_k M_l \text{Tr} P_m M_n = \frac{1}{2} \sum_{k,l} \text{Tr} P_k M_k \text{Tr} P_l M_l. \quad (2.15)$$

Having these expressions, the final ingredient is to compute the static quark propagator  $(1 - T)^{-1}$ , appearing in eq. (2.10).

### 2.4 Static quark propagator

Since  $(1 + \gamma_\mu)(1 - \gamma_\mu) = 0$ , hops in forward and backward time direction do not mix and the full static quark propagator is given by

$$(Q_{\text{stat}})^{-1} = (Q_{\text{stat}}^+)^{-1} + (Q_{\text{stat}}^-)^{-1} - 1.$$

In order to compute the positive static quark propagator, we use the series expansion

$$(Q_{\text{stat}}^+)^{-1} = (1 - T^+)^{-1} = \sum_{n=0}^{\infty} (T^+)^n ,$$

where convergence is only guaranteed for  $z \equiv 2\kappa e^{a\mu} < 1$ . The inverse is given by

$$(Q_{\text{stat}}^+)^{-1}_{\tau_1 \tau_2} = \delta_{\tau_1 \tau_2} (1 - qcW) + qz^{\tau_2 - \tau_1} W(\tau_1, \tau_2) \left[ \Theta(\tau_2 - \tau_1) - z^{N\tau} \Theta(\tau_1 - \tau_2) \right] ,$$

where

$$q \equiv \frac{1}{2} (1 + \gamma_0) (1 + cW)^{-1} ,$$

and  $W(\tau_1, \tau_2)$  is a temporal Wilson line from  $\tau_1$  to  $\tau_2$ . If  $\tau_1 = \tau_2$ , i.e. the Wilson loop winds around the lattice, we have the usual (untraced) Polyakov loop  $W(\tau_1, \tau_1) = W$ . Although we have derived this expression with a geometric series, which converges only for  $c < 1$ , it can be shown that this is indeed the inverse for all values of  $c$ , e.g. by evaluating that  $(Q_{\text{stat}}^+)^{-1} (Q_{\text{stat}}^+) = 1$ .

The contribution in negative time direction  $(Q_{\text{stat}}^-)^{-1}_{\tau_1 \tau_2}$  can then be obtained from  $(Q_{\text{stat}}^+)^{-1}_{\tau_1 \tau_2}$  by the following replacements

$$\tau_1 \leftrightarrow \tau_2 , \quad W(\tau_1, \tau_2) \leftrightarrow W^\dagger(\tau_1, \tau_2) , \quad \mu \leftrightarrow -\mu ,$$

and reads

$$(Q_{\text{stat}}^-)^{-1}_{\tau_1 \tau_2} = \delta_{\tau_1 \tau_2} (1 - \bar{q}\bar{c}W^\dagger) + \bar{q}\bar{z}^{\tau_1 - \tau_2} W^\dagger(\tau_1, \tau_2) \left[ \Theta(\tau_1 - \tau_2) - \bar{z}^{N\tau} \Theta(\tau_2 - \tau_1) \right] ,$$

$$\bar{q} = \frac{1}{2} (1 - \gamma_0) (1 + \bar{c}W^\dagger)^{-1} , \quad \bar{z} = 2\kappa e^{-a\mu} .$$

Finally we split the temporal quark propagator in spin space as well as in propagation in positive and negative temporal direction according to

$$(Q_{\text{stat}})^{-1} = A + \gamma_0 B = A^+ + \gamma_0 B^+ + A^- - \gamma_0 B^- , \quad (2.16)$$

$$A_{xy}^+ = \frac{1}{2} \left[ 1 - \frac{cW}{1 + cW} \right] \delta_{xy} + \frac{1}{2} z^{\tau_y - \tau_x} \frac{W(\tau_x, \tau_y)}{1 + cW} \left[ \Theta(\tau_y - \tau_x) - c\Theta(\tau_x - \tau_y) \right] \delta_{xy} ,$$

$$B_{xy}^+ = -\frac{1}{2} \frac{cW}{1 + cW} \delta_{xy} + \frac{1}{2} z^{\tau_y - \tau_x} \frac{W(\tau_x, \tau_y)}{1 + cW} \left[ \Theta(\tau_y - \tau_x) - c\Theta(\tau_x - \tau_y) \right] \delta_{xy} ,$$

$$A_{xy}^- = \frac{1}{2} \left[ 1 - \frac{\bar{c}W^\dagger}{1 + \bar{c}W^\dagger} \right] \delta_{xy} + \frac{1}{2} \bar{z}^{\tau_x - \tau_y} \frac{W^\dagger(\tau_x, \tau_y)}{1 + \bar{c}W^\dagger} \left[ \Theta(\tau_x - \tau_y) - \bar{c}\Theta(\tau_y - \tau_x) \right] \delta_{xy} ,$$

$$B_{xy}^- = -\frac{1}{2} \frac{\bar{c}W^\dagger}{1 + \bar{c}W^\dagger} \delta_{xy} + \frac{1}{2} \bar{z}^{\tau_x - \tau_y} \frac{W^\dagger(\tau_x, \tau_y)}{1 + \bar{c}W^\dagger} \left[ \Theta(\tau_x - \tau_y) - \bar{c}\Theta(\tau_y - \tau_x) \right] \delta_{xy} ,$$

Due to the length of these terms, we will formulate our results usually in  $A$  and  $B$  for brevity.

## 2.5 The leading correction terms

Now it is time to perform the group integrations. Let us for notational convenience define the following quantities

$$\int [dU_k] \det[Q_{\text{kin}}] \equiv 1 + \sum_{n,m} \Delta^{(n,m)} , \quad (2.17)$$

where  $n$  denotes the order in the hopping parameter  $\kappa$  and  $m$  specifies the  $m$ th term appearing in eqs (2.12-2.15).

### 2.5.1 TrPM:

From eq. (2.12) and after a few steps of algebra the correction of  $\mathcal{O}(\kappa^2)$  is given by

$$\begin{aligned}\Delta^{(2,1)} &\equiv \int [dU_k] \sum_i \text{Tr} P_i M_i = \sum_i \int [dU_k] \text{Tr} \left[ (Q_{\text{stat}}^+)^{-1} S_i^+ (Q_{\text{stat}}^+)^{-1} S_i^- \right] \\ &= -\frac{8\kappa^2}{N_c} \sum_{u,i} \text{Tr} B_{u,u} \text{Tr} B_{u+\hat{i},u+\hat{i}} \\ &= -\frac{2\kappa^2 N_\tau}{N_c} \sum_{\vec{x},i} \left[ \left( \text{Tr} \frac{cW_{\vec{x}}}{1+cW_{\vec{x}}} - \text{Tr} \frac{\bar{c}W_{\vec{x}}^\dagger}{1+\bar{c}W_{\vec{x}}^\dagger} \right) \left( \text{Tr} \frac{cW_{\vec{x}+\hat{i}}}{1+cW_{\vec{x}+\hat{i}}} - \text{Tr} \frac{\bar{c}W_{\vec{x}+\hat{i}}^\dagger}{1+\bar{c}W_{\vec{x}+\hat{i}}^\dagger} \right) \right]\end{aligned}$$

where we have used the expressions eq. (2.16) for  $B$  and evaluated the trace over spin and coordinate space. The group integrations have been computed via

$$\int dU U_{ij} U_{kl}^\dagger = \frac{1}{3} \delta_{il} \delta_{jk}. \quad (2.18)$$

Note that this enforces the spatial link variables to be at the same temporal location and yields a factor  $N_\tau$  rather than  $N_\tau^2$  from the two temporal traces. From now on we will skip the last step, where one has to insert the definitions of  $A$  and  $B$  and perform the temporal sums.

### 2.5.2 TrPPMM:

Here we have three contributions according to eq. (2.13), which after group integration and tracing read

$$\begin{aligned}\Delta^{(4,1)} &= -\frac{32\kappa^4}{N_c^2} \sum_{u,v,i} \text{Tr} B_{u,u} \text{Tr} A_{u+\hat{i},v+\hat{i}} A_{v+\hat{i},u+\hat{i}} \text{Tr} B_{u+2\hat{i},u+2\hat{i}}, \\ \Delta^{(4,2)} &= \mathcal{O}(\kappa^4 u), \\ \Delta^{(4,3)} &= -\frac{16\kappa^4}{N_c^2} \sum_{u,v,i \neq j} \text{Tr} B_{u-\hat{i},u-\hat{i}} \left[ \text{Tr} A_{u,v} A_{v,u} + \text{Tr} B_{u,v} B_{v,u} \right] \text{Tr} B_{u+\hat{j},u+\hat{j}},\end{aligned}$$

where in case of  $\Delta^{(4,2)}$  one has to leave the strong coupling limit and include an additional gauge plaquette due to otherwise vanishing group integration.

### 2.5.3 TrPMPM:

The contributions in this term read following eq. (2.14)

$$\begin{aligned}
\Delta^{(4,4)} &= -\frac{16\kappa^4}{N_c^2} \sum_{u \neq v, i} \left[ \text{Tr} B_{u,v} B_{v,u} \left( \text{Tr} B_{u+\hat{i}, u+\hat{i}} \right)^2 + \left( \text{Tr} B_{u,u} \right)^2 \text{Tr} B_{u+\hat{i}, v+\hat{i}} B_{v+\hat{i}, u+\hat{i}} \right] \\
&\quad - \frac{16\kappa^4}{(N_c^2 - 1)} \sum_{u, i} \left\{ \text{Tr} B_{u,u} B_{u,u} \left( \text{Tr} B_{u+\hat{i}, u+\hat{i}} \right)^2 + \left( \text{Tr} B_{u,u} \right)^2 \text{Tr} B_{u+\hat{i}, u+\hat{i}} B_{u+\hat{i}, u+\hat{i}} \right. \\
&\quad \left. - \frac{1}{N_c} \left[ \text{Tr} B_{u,u} B_{u,u} \text{Tr} B_{u+\hat{i}, u+\hat{i}} B_{u+\hat{i}, u+\hat{i}} + \left( \text{Tr} B_{u,u} \right)^2 \left( \text{Tr} B_{u+\hat{i}, u+\hat{i}} \right)^2 \right] \right\}, \\
\Delta^{(4,5)} &= -\frac{8\kappa^4}{N_c^2} \sum_{u, v, i \neq j} \text{Tr} B_{u-\hat{i}, u-\hat{i}} \left[ \text{Tr} A_{u,v} A_{v,u} + \text{Tr} B_{u,v} B_{v,u} \right] \text{Tr} B_{u+\hat{j}, u+\hat{j}}, \\
\Delta^{(4,6)} &= -\frac{8\kappa^4}{N_c^2} \sum_{u, v, i \neq j} \text{Tr} B_{u-\hat{i}, u-\hat{i}} \left[ \text{Tr} A_{u,v} A_{v,u} + \text{Tr} B_{u,v} B_{v,u} \right] \text{Tr} B_{u-\hat{j}, u-\hat{j}},
\end{aligned}$$

In the calculation of  $\Delta^{(4,4)}$  it may happen that there is a spatial link which is occupied by four matrices and we need the group integral (see e.g. [15])

$$\begin{aligned}
\int dU U_{i_1 j_1} U_{i_2 j_2} U_{k_1 l_1}^\dagger U_{k_2 l_2}^\dagger &= \frac{1}{N_c^2 - 1} \left[ \delta_{i_1 l_1} \delta_{i_2 l_2} \delta_{j_1 k_1} \delta_{j_2 k_2} + \delta_{i_1 l_2} \delta_{i_2 l_1} \delta_{j_1 k_2} \delta_{j_2 k_1} \right] \\
&\quad - \frac{1}{N_c(N_c^2 - 1)} \left[ \delta_{i_1 l_2} \delta_{i_2 l_1} \delta_{j_1 k_1} \delta_{j_2 k_2} + \delta_{i_1 l_1} \delta_{i_2 l_2} \delta_{j_1 k_2} \delta_{j_2 k_1} \right]. \quad (2.19)
\end{aligned}$$

### 2.5.4 (TrPM)<sup>2</sup>:

Here we have to consider two different possibilities: The two nearest-neighbour contributions may share 0, 1 or 2 sites, where the first two lead to the same result. Their contribution is given by

$$\Delta^{(4,7)} = \frac{32\kappa^4}{N_c^2} \sum_{u, v, (u+\hat{i} \neq v+\hat{j})} \text{Tr} B_{u,u} \text{Tr} B_{u+\hat{i}, u+\hat{i}} \text{Tr} B_{v,v} \text{Tr} B_{v+\hat{j}, v+\hat{j}}.$$

The other possibility is that  $(\vec{u}, i) = (\vec{v}, j)$ , i.e. we have only two sites involved and get

$$\begin{aligned}
\Delta^{(4,8)} &= \frac{32\kappa^4}{N_c^2} \sum_{u \neq v, i} \left[ \left( \text{Tr} B_{u,u} \right)^2 \left( \text{Tr} B_{v+\hat{i}, v+\hat{i}} \right)^2 + \text{Tr} B_{u,v} B_{v,u} \text{Tr} B_{u+\hat{i}, v+\hat{i}} B_{v+\hat{i}, u+\hat{i}} \right] \\
&\quad + \frac{32\kappa^4}{N_c^2 - 1} \sum_{u, i} \left\{ \left( \text{Tr} B_{u,u}(\vec{x}) \right)^2 \left( \text{Tr} B_{u+\hat{i}, u+\hat{i}} \right)^2 + \text{Tr} B_{u,u} B_{u,u} \text{Tr} B_{u+\hat{i}, u+\hat{i}} B_{u+\hat{i}, u+\hat{i}} \right. \\
&\quad \left. - \frac{1}{N_c} \left[ \text{Tr} B_{u,u} B_{u,u} \left( \text{Tr} B_{u+\hat{i}, u+\hat{i}} \right)^2 + \left( \text{Tr} B_{u,u} \right)^2 \text{Tr} B_{u+\hat{i}, u+\hat{i}} B_{u+\hat{i}, u+\hat{i}} \right] \right\}.
\end{aligned}$$



**Figure 1:** Finite gauge coupling corrections to the Polyakov line. After spatial link integration these graphs give rise to terms  $\sim \text{Tr}W$ .

## 2.6 Resummations

In order to include as many terms as possible and improve convergence we perform a resummation. The contributions of  $\text{Tr}PM$  and parts of  $\frac{1}{2}\text{Tr}PM\text{Tr}PM$  can be written as an exponential:

$$\begin{aligned} \exp \left[ \Delta^{(2,1)} \right] &= 1 - \frac{8\kappa^2}{N_c} \sum_{u,i} \text{Tr} B_{u,u} \text{Tr} B_{u+i,u+i} \\ &\quad + \frac{32\kappa^4}{N_c^2} \sum_{u,v,i,j} \text{Tr} B_{u,u} \text{Tr} B_{u+i,u+i} \text{Tr} B_{v,v} \text{Tr} B_{v+j,v+j} + \dots \end{aligned} \quad (2.20)$$

Inspection of higher order terms indicates that this should always be possible. Therefore we may write

$$\int [dU_k] \det[Q_{\text{kin}}] = e^{\sum_{n,m} \Delta^{(n,m)}}, \quad (2.21)$$

where  $\Delta^{(4,7)}$  and the parts of  $\Delta^{(4,8)} \sim (\Delta^{(2,1)})^2$  are to be excluded to avoid double counting.

## 2.7 Leading gauge corrections to the strong coupling limit

Leaving the strong coupling limit, i.e.  $\beta \neq 0$ , gauge plaquettes have to be included. This makes the effective coupling constants depend on the gauge coupling:  $h_i(\kappa) \rightarrow h_i(\kappa, u)$ . A somewhat special role plays the single Polyakov line coupling  $c$  introduced in eq. (2.9), since it also enters in the static propagator eq. (2.16). Hence we may further resum terms by replacing the static version  $c$  with  $h_1$ , which is defined to include gauge interactions. The leading gauge corrections are of order  $N_\tau \kappa^2 u$  coming from attaching plaquettes to the Wilson line, cf. fig. 1

$$c \rightarrow h_1 = c \left[ 1 + 6\kappa^2 N_\tau u + \mathcal{O}(\kappa^2 u^5) \right]. \quad (2.22)$$

This can also be exponentiated by summing over multiple attached plaquettes at different locations

$$h_1 = c \exp \left[ 6\kappa^2 N_\tau \frac{u - u^{N_\tau}}{1 - u} \right] = \exp \left[ N_\tau \left( a\mu + \ln 2\kappa + 6\kappa^2 \frac{u - u^{N_\tau}}{1 - u} \right) \right], \quad (2.23)$$

and we see that in this way the Polyakov line receives mass corrections due to interactions. Note that this generates overcounting in higher orders, but in our opinion the resummation effects of this procedure more than compensates for this additional care. Let us finally also give a correction for the coefficient in  $\Delta^{(2,1)}$

$$\frac{2\kappa^2 N_\tau}{N_c} \rightarrow \frac{2\kappa^2 N_\tau}{N_c} \left[ 1 + 2 \frac{u - u^{N_\tau}}{1 - u} + \dots \right]. \quad (2.24)$$



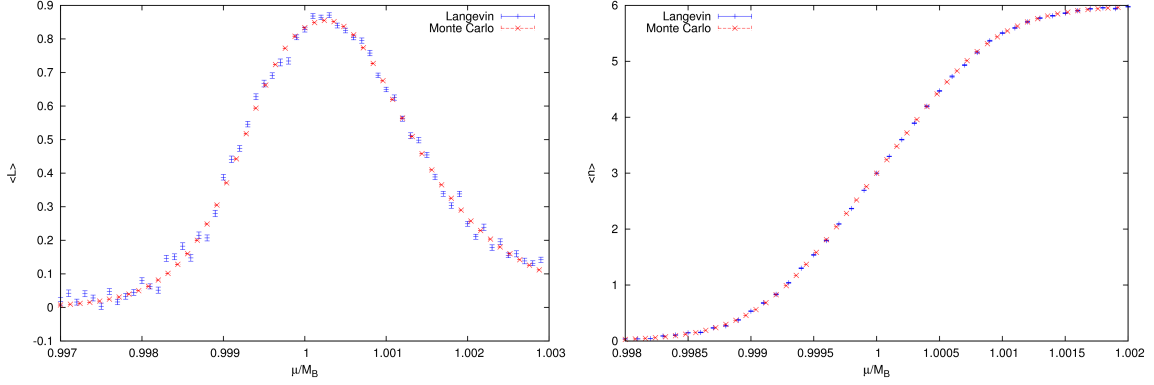


**Figure 2:** Comparison between Langevin and Monte Carlo data at  $\kappa = 0.01$  and  $N_\tau = 200$  in the strong coupling limit.

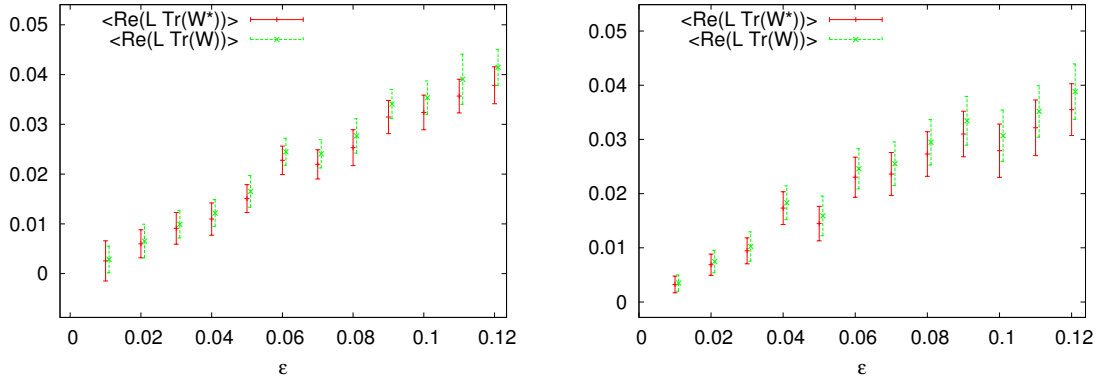


**Figure 3:** Test of the convergence criterion for complex Langevin in the effective theory to order  $\kappa^2$  (left) and  $\kappa^4$  (right) for  $\frac{\kappa^2 N_\tau}{N_c} = 0.01$  and  $\beta = 5.7$ .  $L$  refers to the operator in (3.6).

With this the effective three-dimensional theory we are going to simulate is finally given by

$$Z_{\text{eff}} = \int [dW] \det[Q_{\text{stat}}] \exp \left[ \Delta^{(2,1)} + \sum_m \Delta^{(4,m)} \right], \quad (2.25)$$

where the sum over  $m$  is restricted in the same way as in eq. (2.21).

### 3. Simulation of the effective theory by complex Langevin

The effective theory specified in the last sections has a sign problem. With less degrees of freedom and the theory being only three-dimensional, the sign problem is milder than in the original theory such that Monte Carlo methods are feasible at finite temperatures and chemical potentials  $\mu/T \lesssim 3$  [11]. If, however, one is interested in cold dense matter in the zero temperature limit, the sign problem becomes strong and Monte Carlo methods fail on large volumes. Fortunately, the effective theory is amenable to simulations using complex Langevin algorithms (for an introductory review, see [16]) and the onset transition to nuclear matter could be demonstrated explicitly for very heavy quarks [12]. In this section we discuss the validity of this approach for the effective theory.

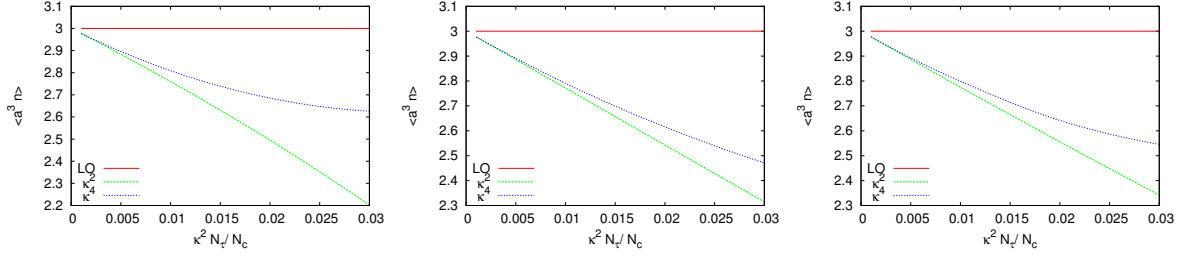


**Figure 4:** Comparison between different orders in  $\kappa$ , using the standard action (left), the resummed action (middle) and including gauge corrections with  $\beta = 6$  (right).

We will only sketch the general method here, as there is an abundant literature on this subject [16, 17, 18].

The basic idea is to introduce a fictitious Langevin time  $\theta$ , in which a field theoretical system with Gaussian noise  $\eta(x, \theta)$  evolves according to the Langevin equation

$$\frac{\partial \phi(x, \theta)}{\partial \theta} = -\frac{\delta S}{\delta \phi(x, \theta)} + \eta(x, \theta). \quad (3.1)$$

In the case of a complex action, the field variables have to be complexified too,  $\phi \rightarrow \phi_r + i\phi_i$ . In our case, after integration over the spatial links, the degrees of freedom are the traced Polyakov lines

$$\int \left[ \prod_{\tau=1}^{N_\tau} dU_0(\tau) \right] f(L, L^*) = \int dW f(L, L^*). \quad (3.2)$$

We may further simplify this by parametrizing the Polyakov lines in terms of two angles and bring them into a diagonal form [20]

$$L(\theta, \phi) = e^{i\theta} + e^{i\phi} + e^{-i(\theta+\phi)}, \quad (3.3)$$

which introduces a potential term denoted by  $e^V$  with

$$V = \frac{1}{2} \ln(27 - 18|L|^2 + 8\text{Re}(L^3) - |L|^4). \quad (3.4)$$

Hence the integration measure we use in our simulation is the reduced Haar measure

$$\int dW = \int dL e^V = \int_{-\pi}^{\pi} d\theta \int_{-\pi}^{\pi} d\phi e^{2V}. \quad (3.5)$$

This means instead of an integration over  $N_\tau$  SU(3) matrices we have 2 complex degrees of freedom on every spatial lattice point. Furthermore, having only diagonal matrices their inversion is trivial. With these ingredients eq.(3.1) was solved numerically using stepsizes of around  $\varepsilon = 10^{-3}$  and applying the adaptive stepsize technique proposed in [21] to avoid numerical instabilities.

### 3.1 Criteria for correctness

Unfortunately, it is well known that the complex Langevin algorithm is not a general solution to the complex action problem as it converges to the wrong limit in some cases, including some

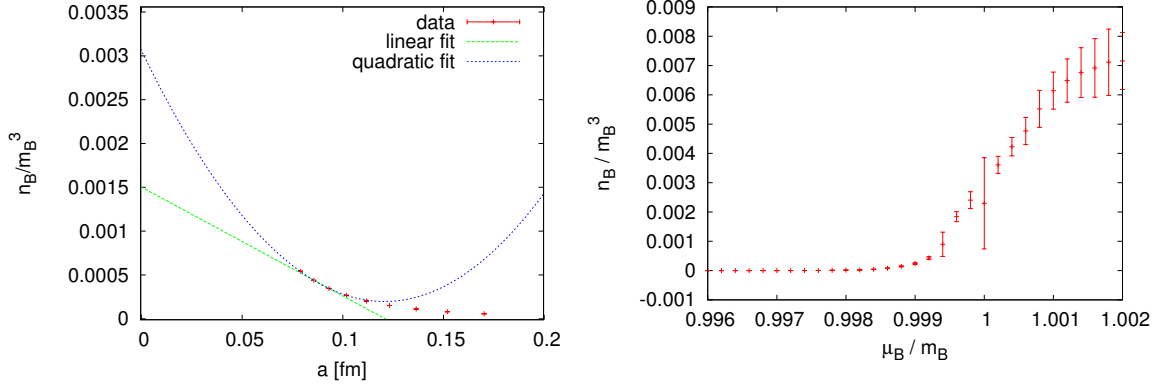


**Figure 5:** Examples for the continuum extrapolation. Shown are linear and quadratic extrapolations with one d.o.f. (left) and continuum extrapolated results for the transition to cold nuclear matter for  $T = 10$  MeV (right). In order to set the scale we use results for  $r_0$  from [22] and the strong coupling and hopping parameter expansion of the baryon mass from [12].

parameter ranges for QCD [16, 19]. The failure can be attributed to insufficient localisation of the probability distribution in the complex field space, and a set of criteria was developed to check whether this localisation is sufficient [17]. A necessary condition is that the expectation value of all observables vanishes after a Langevin operator  $\hat{L}$  has been applied to them,

$$\langle \hat{L}O[\phi] \rangle = 0, \quad \hat{L} = \sum_{a,x} \left( \frac{\partial}{\partial \phi_a(x)} - \frac{\partial S}{\partial \phi_a(x)} \right) \frac{\partial}{\partial \phi_a(x)}. \quad (3.6)$$

While, strictly speaking, this test is necessary on *all* observables of the theory, in practice only a select few can be tested. In figure 3 we show the expectation value of the Polyakov loop as a function of the step size of the Langevin algorithm for the effective theory to order  $\kappa^2$  (left) and  $\kappa^4$  (right). In both cases the criterion is fulfilled.

As a further and complementary check of the validity of the complex Langevin simulation, we also compare with reweighted Monte Carlo results where this is possible, i.e. on small volumes. As figure 2 shows, this test is also passed by the complex Langevin data for the expectation value of the Polyakov loop as well as the baryon number density.

### 3.2 Convergence region of the hopping series

One of the most important values we want to determine is the region of convergence of the effective theory. This is the region where the truncated theory is a good approximation to the full theory. As criteria for convergence we choose the difference between expectation values obtained from the  $\kappa^2$  and the  $\kappa^4$  action for different values of the expansion parameter  $\frac{\kappa^2 N_c}{N_c}$ . The expansion parameter already shows that the region of convergence is limited in the direction of low temperatures and light quarks, i.e. one can reach lower quark masses by raising the temperature. As an observable we choose the density in lattice units  $\langle a^3 n \rangle$  with a chemical potential chosen such that  $h_1(\kappa, u, \mu) = 1$ . As can be seen in figure 4 the static limit is only a valid approximation in the  $\kappa \rightarrow 0$  limit. If we define the limit of the region of convergence as a certain value of the difference between  $\langle a^3 n \rangle_{\kappa^2}$  and  $\langle a^3 n \rangle_{\kappa^4}$  one can see that the resummed action offers a better convergence. Therefore, we will use this version for our simulations.

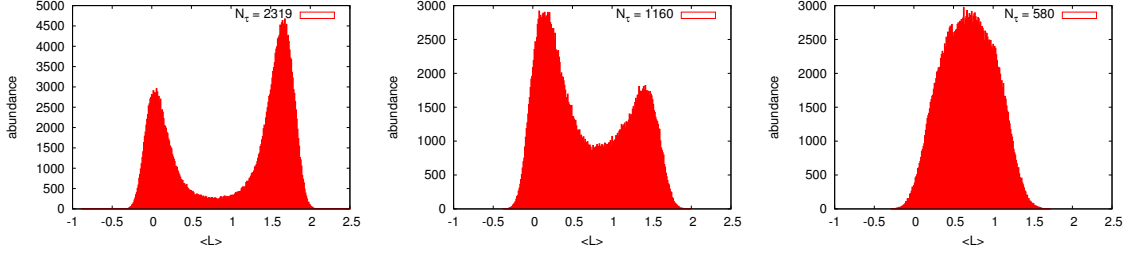


**Figure 6:** Polyakov Loop histograms in the transition region for three different temperatures,  $\kappa = 0.12$  and  $\beta = 5.7$ .

### 3.3 Silver blaze property and onset to nuclear matter

In our previous work [12] we performed a continuum extrapolation for the transition to cold nuclear matter based on the  $\kappa^2$  action. In figure 4 we repeat this calculations including the  $\kappa^4$  corrections. This allows us to simulate smaller lattice spacings  $a = 0.08$  fm without leaving the region of convergence, since reducing  $a$  while keeping  $\frac{M}{T}$  fixed means going to higher  $\kappa$ . Nevertheless the extrapolation suffers from considerable uncertainties, resulting in large errors in the high density phase. This can be seen in fig. 5 (left), where we show the two best fits for our data at  $\frac{\mu}{m_B} = 1$  at several lattice spacings. This is the chemical potential where different extrapolation fits differ the most. The truncation error for our  $\kappa^4$  data is estimated as the difference to the data obtained from the  $\kappa^2$  action. This data was then fitted to get a value for  $a \rightarrow 0$ .

As continuum result we took the average of the two best fits, the error was estimated as difference between those two fits. For each value of the chemical potential we tried several fits (linear and quadratic) with one to three degrees of freedom. For the best fits we always achieved  $\chi_{red}^2 < 2$  as long as  $\frac{m_{UB}}{m_B} < 1.0014$ . The growing uncertainties in the high density region are caused by the unphysical saturation on the lattice which limits the density to  $2N_c$  quarks per lattice site, while in the continuum no such saturation exists. In the low density region the Silver Blaze property, i.e. the independence from chemical potential in the  $T \rightarrow 0$  limit below a critical value  $\mu_c$ , can be seen. Note that the results at  $\kappa^4$  are somewhat higher than our  $\kappa^2$ -results in [12]. The inclusion of  $\kappa^4$  allows for a better estimate of the truncation error and therefore inclusion of data from lattices with smaller lattice spacing.

As in our previous work [12], the accessible quark masses in the convergence region of the effective theory are too high to realize the expected first order transition from the vacuum to the region of finite density, i.e. the transition proceeds as a smooth crossover. However, this changes if we leave the convergence region by going to lower quark masses ( $\kappa = 0.12$ ) and very low temperatures with  $N_\tau = O(10^3)$ , where we see signals for a first order transition. Figure 6 shows distributions of Polyakov Loop expectation values in the transition region. It clearly shows coexistence of two distinct phases, i.e. the effective action describes a first order transition which disappears as temperature is raised ( $N_\tau$  is lowered). However, in order to make quantitative statements we will have to extend the region of convergence by adding several higher orders in  $\kappa$ .

## Acknowledgements

J.L. is supported by the Swiss National Science Foundation under grant 200020-137920. M.N. and O.P. are supported by the German BMBF, grant 06FY7100, and the Helmholtz International Center for FAIR within the LOEWE program launched by the State of Hesse.

## References

- [1] P. de Forcrand, PoS LAT **2009** (2009) 010 [arXiv:1005.0539 [hep-lat]].
- [2] G. Aarts, PoS LATTICE **2012** (2012) 017 [arXiv:1302.3028 [hep-lat]].
- [3] G. Aarts, L. Bongiovanni, E. Seiler, D. Sexty and I. -O. Stamatescu, Eur. Phys. J. A **49** (2013) 89 [arXiv:1303.6425 [hep-lat]].
- [4] C. Gattringer and T. Kloiber, Nucl. Phys. B **869** (2013) 56 [arXiv:1206.2954 [hep-lat]].
- [5] Y. D. Mercado, C. Gattringer and A. Schmidt, Comput. Phys. Commun. **184** (2013) 1535 [arXiv:1211.3436 [hep-lat]].
- [6] M. Cristoforetti *et al.* [AuroraScience Collaboration], Phys. Rev. D **86** (2012) 074506 [arXiv:1205.3996 [hep-lat]].
- [7] W. Unger and P. de Forcrand, J. Phys. G **38** (2011) 124190 [arXiv:1107.1553 [hep-lat]].
- [8] M. Fromm, J. Langelage, O. Philipsen, P. de Forcrand, W. Unger and K. Miura, PoS LATTICE **2011** (2011) 212 [arXiv:1111.4677 [hep-lat]].
- [9] N. Kawamoto, K. Miura, A. Ohnishi and T. Ohnuma, Phys. Rev. D **75** (2007) 014502 [hep-lat/0512023].
- [10] T. Z. Nakano, K. Miura and A. Ohnishi, Phys. Rev. D **83** (2011) 016014 [arXiv:1009.1518 [hep-lat]].
- [11] M. Fromm, J. Langelage, S. Lottini and O. Philipsen, JHEP **1201** (2012) 042 [arXiv:1111.4953 [hep-lat]].
- [12] M. Fromm, J. Langelage, S. Lottini, M. Neuman and O. Philipsen, Phys. Rev. Lett. **110** (2013) 122001 [arXiv:1207.3005 [hep-lat]].
- [13] J. Langelage, S. Lottini and O. Philipsen, JHEP **1102** (2011) 057 [Erratum-ibid. **1107** (2011) 014] [arXiv:1010.0951 [hep-lat]].
- [14] J. Langelage, S. Lottini and O. Philipsen, PoS LATTICE **2010** (2010) 196 [arXiv:1011.0095 [hep-lat]].
- [15] M. Creutz, J. Math. Phys. **19** (1978) 2043.
- [16] P. H. Damgaard and H. Hüffel, Phys. Rept. **152**, 227 (1987).
- [17] G. Aarts, F. A. James, E. Seiler and I. -O. Stamatescu, Eur. Phys. J. C **71**, 1756 (2011) [arXiv:1101.3270 [hep-lat]].
- [18] G. Aarts and F. A. James, JHEP **1201**, 118 (2012) [arXiv:1112.4655 [hep-lat]].
- [19] J. Ambjorn, M. Flensburg and C. Peterson, Nucl. Phys. B **275** (1986) 375.
- [20] M. Gross, J. Bartholomew and D. Hochberg, Report No. EFI-83-35-CHICAGO, 1983
- [21] G. Aarts, F. A. James, E. Seiler and I. -O. Stamatescu, Phys. Lett. B **687** (2010) arXiv:0912.0617 [hep-lat].
- [22] S. Necco and R. Sommer, Nucl. Phys. B **622** (2002) 328 [hep-lat/0108008].